DYNAMIC RESPONSE OF REACTOR CONTAINMENT TO HIGH-ENERGY EXCURSION*

Y.-W. CHANG, J. GVILDYS,

Reactor Analysis and Safety Division, Argonne National Laboratory, Argonne, Illinois, U.S.A.

ABSTRACT

This paper describes a numerical method for calculating the dynamic response of a primary reactor containment system to a high-energy excursion. Media inside the reactor containment are treated as compressible fluids. Hydrodynamic equations and equations of state of reactor materials are used for calculating the propagation of shock waves emanating from the reactor core, the loads imposed on adjacent structures and components, the damage produced by these loads, and the motion of the coolant. Plate-shell equations are used to determine the dynamic response of the reactor containment in which the containment material is considered to be elastic-plastic, strain-hardening and strain-rate sensitive. In the analysis, all equations are expressed in material coordinates and then set into numerical form by finite-difference equations. Shock discontinuities are eliminated by the introduction of an artificial viscosity. The numerical solution of these finite-difference equations is done on the IBM-360 computer, using the REXCO-H code developed at Argonne National Laboratory.

1. INTRODUCTION

Large, liquid-metal-cooled, fast reactors probably cannot be designed to completely rule out the possibility of a core meltdown. Therefore, the reactor designer must rigorously analyze the capability of the primary containment system to sustain the consequences of such an accident. To accomplish this objective, he must know in detail the propagation of shock waves emanating from the reactor core, the loads imposed on adjacent structures and components, and the damage produced by these loads. Most important, he must know the dynamic response of the reactor containment.

This paper describes a numerical method for calculating the two-dimensional dynamic response of a primary reactor containment system to a high-energy excursion in the core. Hydrodynamic equations and equations of state of reactor materials are used for calculating the propagation of shock waves emanating from the reactor core, the loads imposed on adjacent structures and components, the damage produced by these loads, and the motion of the coolant. Plate-shell equations are used to determine the dynamic response of the reactor containment in which the containment material is considered to be elastic-plastic, strain-hardening and

* This work performed under the auspices of the U.S. Atomic Energy Commission.

strain-rate sensitive. This approach offers a number of advantages over conventional methods based upon chemical explosion and scaled model, including: (1) ability to simulate nuclear excursion conditions so that containment response is determined directly from postulated accident conditions; (2) ability to use a more refined analytical model; (3) ability to vary a single parameter so that its independent effect can be studied; (4) ability to determine the sequence of a component failure and its effect on loads imposed on the reactor containment; and (5) considerably lower cost and less time.

In the analysis, all equations are expressed in material coordinates and then set into numerical form by finite-difference equations. Shock discontinuities are eliminated by the introduction of an artificial viscosity. The hydrodynamics and containment response calculations are done separately in two finite-difference calculations. Each maintains its own integrity but interact, every cycle, by supplying each other's required boundary condition along the common boundary. For containment response, it uses a pressure versus time and position boundary condition obtained from the hydrodynamics calculation, whereas for the hydrodynamics it uses a displacement versus time and position boundary condition supplied by the containment response calculation. The numerical solution of these finite-difference equations is done on the IBM-360 computer, using the REXCO-H code developed at Argonne National Laboratory.*

2. ANALYTICAL DEVELOPMENT

2.1. Hydrodynamic Equations of Shock Waves

2.1.1. Basic Equations

The partial differential equations that govern the flow of a nonviscous, non-heat-conducting, compressible fluid are

$$\frac{D\rho}{Dt} + \rho \operatorname{div} \bar{u} = 0 \quad \text{(mass)}$$

$$\rho \frac{D\bar{u}}{Dt} = -\operatorname{grad} p \quad \text{(momentum)}$$

$$\frac{DE}{Dt} + p \frac{DV}{Dt} = 0 \quad \text{(energy)}$$

where $\frac{D}{Dt}$ is the total derivative, $\bar{u}$ is the velocity vector, ρ is the density, p is the pressure, E is the specific internal energy, and V is the specific volume. It is assumed that there are no external energy sources in the fluid. If the flow is axially symmetric, the above equations take the form

$$\frac{\partial \rho}{\partial t} + u \frac{\partial \rho}{\partial r} + w \frac{\partial \rho}{\partial z} = -\rho \left(\frac{\partial u}{\partial r} + \frac{\partial w}{\partial z} + \frac{u}{r} \right) \tag{1}$$

---

* A power-excursion computer code, also developed at Argonne, provides initial values for the REXCO-H code. Both codes will be linked in sequence, constituting two modules of the Postburst Phenomena of the Fast Reactor Safety Program.

$$\frac{\partial u}{\partial t} + u \frac{\partial u}{\partial r} + w \frac{\partial u}{\partial z} = - \frac{1}{\rho} \frac{\partial p}{\partial r} \tag{2}$$

$$\frac{\partial w}{\partial t} + u \frac{\partial w}{\partial r} + w \frac{\partial w}{\partial z} = - \frac{1}{\rho} \frac{\partial p}{\partial z} \tag{3}$$

$$\frac{\partial E}{\partial t} + u \frac{\partial E}{\partial r} + w \frac{\partial E}{\partial z} = -p\left(\frac{\partial V}{\partial t} + u \frac{\partial V}{\partial r} + w \frac{\partial V}{\partial z}\right) \tag{4}$$

Here r and z are the cylindrical coordinates, u and w are the radial and axial velocities, respectively. Eqs. (1) to (4) are the Eulerian formulation of the fluid dynamics in which the independent space variables are referred to a coordinate system fixed in space. The alternative is to express the equations in material coordinates, and these equations are known as the Lagrangian equations of the fluid dynamics.

In Lagrangian formulation, the equation of mass conservation is simply

$$\frac{\rho_0}{\rho} = \frac{dv}{dV} \tag{5}$$

where ρ_0 is the initial density at time t = 0, and dv and dV are the volume elements in the deformed and undeformed states, respectively. The momentum equations become

$$\ddot{r} = - \frac{1}{\rho_0}\left(\frac{\partial p}{\partial R}\frac{\partial z}{\partial Z} - \frac{\partial p}{\partial Z}\frac{\partial z}{\partial R}\right)\frac{r}{R}$$

$$\ddot{z} = \frac{1}{\rho_0}\left(\frac{\partial p}{\partial R}\frac{\partial r}{\partial Z} - \frac{\partial p}{\partial Z}\frac{\partial r}{\partial R}\right)\frac{r}{R}$$

where R and Z are the Lagrangian coordinates.

Although ρ_0, ∂R, and ∂Z are independent of time, the momentum equations have become considerably more complicated by the transformation. In the numerical analysis, it was easier to work with the quantities ρ, ∂r, and ∂z directly. Therefore, the equations used are of the form

$$\ddot{r} = - \frac{1}{\rho}\frac{\partial p}{\partial r} \tag{6}$$

$$\ddot{z} = - \frac{1}{\rho}\frac{\partial p}{\partial z} \tag{7}$$

where r and z are dependent variables; they are functions of (R,Z,t). Each fluid particle is now labeled with a set of Lagrangian coordinates [R(I),Z(J)]. Since the Lagrangian coordinates are imbedded in the fluid particle and move with the fluid, the total derivative is simply the time derivative, and the energy equation reduces to

$$dE = -pdV \tag{8}$$

Eqs. (5) to (8) are the hydrodynamic equations in the Lagrangian formulation. There are five unknowns: density of the fluid, ρ; radial and axial accelerations of the fluid, $\ddot{r}$ and

$\ddot{z}$; pressure in the fluid, p; and specific internal energy, E. To obtain a unique solution, a fifth equation relating the various unknowns is needed. If the thermodynamic properties of the fluid are known, a relationship between p, E, and ρ can be established. Such a relationship is known as the equation of state of the fluids. In the present analysis, this equation is assumed to have the form

$$p = f(V,E) \tag{9}$$

Eqs. (5) to (9) apply only to the smooth part of the flow, i.e., without shocks, or the flow between shocks. For flows at the shocks, the dependent variables (ρ, u, w, E, and p) are no longer continuous: the differential equations at the shock only have one-sided derivatives. Therefore, they must be supplemented by jump conditions that serve as internal boundary conditions. These special boundary conditions are provided by the well-known Rankine-Hugoniot equations. However, their application is complicated by the fact that the surfaces on which the conditions are to be applied are in motion through the fluid and that the motion of the surfaces is determined by the equations themselves.

2.1.2. Elimination of Shock Discontinuities

To avoid the above-mentioned complication, von Neumann and Richtmyer [1] devised an approximate method for solving one-dimensional fluid-dynamics problems that eliminates discontinuities in the differential equations and dampens out spurious pressure oscillations in the numerical computations. Their method uses the well-known effect of dissipative mechanisms, such as viscosity and heat of conduction, on shocks. For example, when viscosity is taken into account, the shocks are smeared out and the mathematical surfaces of the discontinuities are replaced by thin transition layers in which quantities such as pressure, temperature, and density vary rapidly but continuously.

Accordingly, von Neumann and Richtmyer introduced a pseudo-viscosity term, q, into the differential equations, thereby eliminating the shock discontinuities without jeopardizing the conservation laws on which the Hugoniot conditions are based. Also, the jump conditions across the transition layer still hold in the approximation in which the layer is regarded as thin, relative to other dimensions.

Here we apply their method into two-dimensional flows. The differential equations employed in the pseudo-viscosity method are

$$\frac{\rho_0}{\rho} = \frac{d\forall}{d\forall}$$

$$\ddot{r} = -\frac{1}{\rho}\left[\frac{\partial(p+q)}{\partial r}\right]$$

$$\ddot{z} = -\frac{1}{\rho}\left[\frac{\partial(p+q)}{\partial z}\right]$$

$$dE = -(p+q)\, dV$$

$$p = f(V,E) \tag{10}$$

The form of q is taken as

$$q = \frac{a^2 \rho_0 A}{V^2}\left(\frac{\partial V}{\partial t}\right)^2 \quad \text{if } \frac{\partial V}{\partial t} < 0$$

$$= 0 \qquad \text{if } \frac{\partial V}{\partial t} \geq 0 \tag{11}$$

where A is the area of the Lagrangian mesh at time t when the fluid density changes to ρ. The value of a that yields the desired shock width ranges from 1.2 to 1.4. Here, a is assumed to be 1.2.

2.2. Equation of State of the Media

As stated in the previous section, solution of the four hydrodynamic equations requires an equation of state of the form given by eq. (9). For gaseous materials, the pressure is of thermal origin; it is related to the transfer of momentum by particles participating in the thermal motion. Therefore, no appreciable difficulties are encountered in calculating the thermodynamic properties of gases. For instance, the vapor pressure of a reactor core can be approximated by the following equation

$$p = A \exp\left(B + \frac{C}{T} + \frac{D}{\ln T}\right) \tag{12}$$

where T is the temperature, and A, B, C, and D are fitting parameters.

In contrast, a theoretical description of similar properties of solids and liquids at high pressures generated by strong shocks presents a complex problem. Here the atoms or molecules are in proximity and interact strongly with each other. Thus, strong compression of a condensed medium generates not only a thermal pressure, but also a significant internal pressure. The internal pressure is due to repulsive forces between the atoms; it differs from the thermal pressure associated with thermal motion of the atoms. Here in this analysis, the equation of state of the condensed material at high pressures is based on the experimental Hugoniot (p_H curve). The equation used is the Mie-Grüneisen equation of state, which may be written

$$p = p_H + \frac{\gamma}{V}(E - E_H) \tag{13}$$

where p_H and E_H are the pressure and specific internal energy along the Hugoniot centered at p_0, V_0; and γ, the Grüneisen coefficient, is the ratio of the thermal component of pressure to the lattice vibrational energy density; it is a function only of volume. The neighboring states are determined from the Hugoniot centered at p_0, V_0 by adding an additional term $(\gamma/V)(E - E_H)$, which acts like a thermal pressure rise.

At low pressures, compression measurements obtained from shock experiments become less reliable. As an alternate, the pressure is evaluated from the bulk modulus and its pressure derivatives using the Murnaghan equation of state [2]

$$p = \frac{B_0}{B_0'}\left[\left(\frac{V_0}{V}\right)^{B_0'} - 1\right] \tag{14}$$

where V and V_0 are the deformed and undeformed volumes, respectively, and B_0 and B_0' are the bulk modulus and its pressure derivative, respectively. In Murnaghan's original derivation, B_0 and B_0' are two constants corresponding to a fixed temperature, usually room temperature. Here, this equation has been generalized to arbitrary temperature by assuming B_0 and B_0' to be temperature-dependent parameters.

2.3. Plate-Shell Equations

The formulation of the equations of dynamic equilibrium of a shell structure is extremely complicated. It has been decided that as a first step, only shells of revolution under rotationally symmetric loadings will be treated. Therefore, the reactor containment vessels considered in this paper are limited to cylindrical shells and circular plates.

Fig. 1.a. shows a shell of revolution defined by the curvilinear coordinates s and θ. The location of any point on the meridian can be determined by the two coordinates r and z. On the element of the shell shown in fig. 1.b., there are two tangential stress resultants N_θ and N_ϕ, a transverse stress resultant Q_ϕ, and two stress couples M_θ and M_ϕ. The equations of equilibrium for large deflections of shells are

$$\frac{\partial}{\partial s}\left[N_\phi r \cos\phi\right] - \frac{\partial}{\partial s}\left[Q_\phi r \sin\phi\right] - N_\theta - mr\ddot{r} = 0 \tag{15}$$

$$\frac{\partial}{\partial s}\left[N_\phi r \sin\phi\right] + \frac{\partial}{\partial s}\left[Q_\phi r \cos\phi\right] - mr\ddot{z} = 0 \tag{16}$$

$$\frac{\partial}{\partial s}\left[M_\phi r\right] - M_\theta \cos\phi - Q_\phi r = 0 \tag{17}$$

where m is the mass of the shell per unit area, and ϕ is the angle of inclination of the element with respect to the r direction. The thickness of the shell is idealized by n discrete layers of material that can carry normal stresses in the planes parallel to the tangential plane of the shell surface, whereas the material connecting these layers cannot carry normal stress but has infinite shear rigidity.

2.4. Constitutive Relations

The constitutive equations permit the determination of the state of stress at any instant in time when the stress at the prior instant and strain increments are known. For the elastic-plastic material, the strain increments may be composed of an elastic and plastic component as follows:

$$\begin{aligned}\Delta\varepsilon_\phi &= \Delta\varepsilon_\phi^{\,e} + \Delta\varepsilon_\phi^{\,p}\\ \Delta\varepsilon_\theta &= \Delta\varepsilon_\theta^{\,e} + \Delta\varepsilon_\theta^{\,p}\end{aligned} \tag{18}$$

where ε_ϕ and ε_θ are the principal plane strains. The elastic strain increments are given by

$$\begin{aligned}\Delta\varepsilon_\phi^{\,e} &= \frac{1}{E}\left(\Delta\sigma_\phi - \nu\Delta\sigma_\theta\right)\\ \Delta\varepsilon_\theta^{\,e} &= \frac{1}{E}\left(\Delta\sigma_\theta - \nu\Delta\sigma_\phi\right)\end{aligned} \tag{19}$$

and the plastic strain increments can be written according to the incremental strain theory of plasticity, as follows:

$$\Delta\varepsilon_{\phi}^{p} = \frac{1}{3}(2\sigma_{\phi} - \sigma_{\theta})\,\Delta\lambda$$

$$\Delta\varepsilon_{\theta}^{p} = \frac{1}{3}(2\sigma_{\theta} - \sigma_{\phi})\,\Delta\lambda \tag{20}$$

where λ is a measure of the plastic deformation. Eq. (18) thus contains three unknown quantities: $\Delta\sigma_{\phi}$, $\Delta\sigma_{\theta}$, and $\Delta\lambda$. A third equation required for the solution is the yield condition. In the present analysis, the Mises-Hencky yield condition is employed; namely

$$(\sigma_{\phi} + \Delta\sigma_{\phi})^2 - (\sigma_{\phi} + \Delta\sigma_{\phi})(\sigma_{\theta} + \Delta\sigma_{\theta}) + (\sigma_{\theta} + \Delta\sigma_{\theta})^2 = \sigma_{o}^{2} \tag{21}$$

where σ_o is the yield stress of the given material under uniaxial stress conditions.

Two other effects are readily incorporated into the constitutive relations. The strain-hardening solid is conveniently represented by using, for example, a model in which the material is decomposed into subregions of elastic, perfectly plastic materials having different yield stresses but common strains. Another effect that can be treated is strain-rate sensitivity. If the primary effect of strain rate on a metal is that the yield stress of the material is raised as the strain rate is increased, then the yield stress σ_y at any instant, at any location may be computed as follows:

$$\sigma_y = \sigma_o \left[1 + \left(\frac{\dot{\varepsilon}}{D}\right)^{\frac{1}{p}}\right] \tag{22}$$

where

$$\dot{\varepsilon} = \left(\frac{4}{3}\right)^{\frac{1}{2}} [\dot{\varepsilon}_{\theta}^{2} + \dot{\varepsilon}_{\phi}^{2} + \dot{\varepsilon}_{\theta}\dot{\varepsilon}_{\phi}]^{\frac{1}{2}} \tag{23}$$

and D, p are material constants.

2.5. Stability of the Differential Equations

Another quantity of particular interest to the numerical solution of differential equations is the criterion for stability of a finite-difference mesh. For media inside the reactor containment White stability criterion is used [3].

$$W = \left[\frac{c^2(\Delta t)^2}{A} + 4a^2\left|\frac{\Delta V}{V}\right|\right]^{\frac{1}{2}} < 1 \tag{24}$$

where W is White stability number, c is the speed of sound, and ΔV is the change of specific volume. To ensure additional computational stability, the value of W is limited to less than 0.45 and greater than 0.2245.

For containment vessel the stability criteria, which determine the selection of the time increment, are:

$$\Delta t \leq \Delta x \left(\frac{\rho}{E}\right)^{\frac{1}{2}}$$

or

$$\Delta t \leq \left(\frac{\Delta x}{2}\right)^2 \left(\frac{\bar{\rho}}{D}\right)^{1/2} \tag{25}$$

where Δx is the mesh size, ρ is the density per unit volume, E is Young's modulus, $\bar{\rho}$ is the mass per unit area of the plate or shell, and D is the flexural rigidity of the shell. Again, to ensure additional computational stability, a time step of 0.80 of the critical value obtained from eq. (25) is used in the numerical computation.

2.6. Finite-difference Equations

2.6.1. Hydrodynamics

Fig. 2 shows a typical mesh point, (I,J), with the adjacent zones and points. The mesh points (the intersections of Lagrangian grid lines) are identified by a pair of integers (I,J). The mesh zones are identified by the integers on the lower left mesh point (in the undeformed Lagrangian meshes); for example, the mesh zone ODHA is identified as zone (I,J). Positions, velocities, and accelerations are assumed to be associated with the mesh points; they are identified by the mesh-point integers as subscripts. Specific volumes, densities, pressures, pseudo-viscosities, strains, internal energies, and White stability numbers are assumed to be associated with zones; they are identified by the zone numbers as subscripts. Time is denoted by t. The times t, $t + \Delta t$, and $t + \frac{\Delta t}{2}$ at which quantities are assumed to be known or calculated are identified by superscripts n, $n + 1$, and $n + \frac{1}{2}$. The latter is also used to identify the change in a quantity between t^n and t^{n+1}. Where appearing, the superscript 0 denotes the initial value of a quantity at the start of the problem.

Since the Lagrangian meshes are used, the mass equation is automatically satisfied. However, this equation is needed for the computation of the new density ρ, which occurs in the momentum equations.

The area of the deformed mesh ODHA is calculated from:

$$A_{I,J} = \frac{1}{2}\Big[(z_{I+1,J+1} - z_{I,J})(r_{I+1,J} - r_{I,J+1}) - (r_{I+1,J+1} - r_{I,J})(z_{I+1,J} - z_{I,J+1})\Big] \tag{26}$$

The volume V of a quadrilateral is calculated from

$$V_{I,J} = A_{I,J} 2\pi \bar{r}_{I,J} \tag{27}$$

where $\bar{r}_{I,J}$ is the radius of the centroid of the area $A_{I,J}$. In Lagrangian coordinates, the mass of each volume is constant with time; therefore, the density of a quadrilateral at time n is obtained by

$$\rho^n_{I,J} = \frac{(\rho_0 V^0)_{I,J}}{V^n_{I,J}} \tag{28}$$

The momentum equations in finite-difference form are

$$\ddot{r}_{I,J} = \frac{-1}{(A\rho)_{I,J}} \left[(P_{I,J} - P_{I-1,J-1})(z_{I,J+1} - z_{I,J-1} + z_{I-1,J} - z_{I+1,J}) - (P_{I-1,J} - P_{I,J-1})(z_{I,J+1} - z_{I,J-1} + z_{I+1,J} - z_{I-1,J}) \right] \quad (29)$$

$$\ddot{z}_{I,J} = \frac{1}{(A\rho)_{I,J}} \left[(P_{I,J} - P_{I-1,J-1})(r_{I,J+1} - r_{I,J-1} + r_{I-1,J} - r_{I+1,J}) - (P_{I-1,J} - P_{I,J-1})(r_{I,J+1} - r_{I,J-1} + r_{I+1,J} - r_{I-1,J}) \right] \quad (30)$$

where $P = p + q$

$$(A\rho)_{I,J} = A_{I,J}\rho_{I,J} + A_{I-1,J}\rho_{I-1,J} + A_{I-1,J-1}\rho_{I-1,J-1} + A_{I,J-1}\rho_{I,J-1}$$

The pressure p and specific internal energy E of each zone are obtained from the equation of state,

$$p^n = f(V^n, E^n) \quad (31)$$

and from the equation of conservation of energy, $dE = -(p + q)\, dV$, in difference form,

$$E^n = E^{n-1} - \frac{1}{2}(P^{n-1} + p^n + q^n)\, \Delta V^{n-\frac{1}{2}} \quad (32)$$

where

$$\Delta V^{n-\frac{1}{2}} = V^n - V^{n-1}$$

The complete derivations of these finite-difference equations are given in refs. [4] and [5].

2.6.2. Containment Response

At high pressures, the mechanical properties of the solid material can be described by using a compressible-fluid model. However, as the material recovers from the shock loading, or the material is under tension, the tensile strength of the material becomes important. This is particularly true in the case of containment vessel, where the radial movement of the shell produces membrane and bending forces and where the tensile strength of the material is the most important mechanism for resisting the motion of the shell. Thus, for containment vessels, the effects of material strength must be included in the formulation of the momentum equations.

(a) Cylindrical Shell

Let the I line in fig. 2. be the middle plane line of the cylindrical shell. The

acceleration in z direction is given by eq. (16), in finite-difference form,

$$\ddot{z}_{I,J} = \frac{1}{m_{57}} \left[N_{\phi_{I,J+\frac{1}{2}}} r_{I,J+\frac{1}{2}} \sin\phi_{I,J} - N_{\phi_{I,J-\frac{1}{2}}} r_{I,J-\frac{1}{2}} \sin\phi_{I,J-1} \right.$$

$$\left. + Q_{\phi_{I,J+\frac{1}{2}}} r_{I,J+\frac{1}{2}} \cos\phi_{I,J} - Q_{\phi_{I,J-\frac{1}{2}}} r_{I,J-\frac{1}{2}} \cos\phi_{I,J-1} \right] \tag{33}$$

where m_{57} is the mass of the shell segment 57, and $\phi_{I,J}$, $\phi_{I,J-1}$ are, respectively, the angle of inclination of the elements OA and CO with respect to the r direction. The acceleration in the r direction is given by

$$\ddot{r}_{I,J} = \frac{-1}{(A_0)_{I,J}} \left[(P_{I,J} - P_{I-1,J-1} + P_3)(z_{I,J+1} - z_{I,J-1} + z_{I-1,J} - z_{I+1,J}) \right.$$

$$\left. - (P_{I-1,J} - P_2 - P_{I,J-1})(z_{I,J+1} - z_{I,J-1} + z_{I+1,J} - z_{I-1,J}) \right] \tag{34}$$

where the strength of the shell is represented by two equivalent pressures P_2 and P_3. If the strength of the shell is ignored, i.e., $P_2=P_3=0$, eq. (34) reduces to eq. (29). The pressures P_2 and P_3 are calculated from

$$P_2 = \frac{N_{\theta_{I,J+\frac{1}{2}}} \sin\phi_{I,J}}{r_{I,J+\frac{1}{2}}} + P_{23}$$

$$P_3 = \frac{N_{\theta_{I,J-\frac{1}{2}}} \sin\phi_{I,J-1}}{r_{I,J-\frac{1}{2}}} + P_{23}$$

$$P_{23} = \frac{1}{\ell_{57} r_{I,J}} \left[N_{\phi_{I,J-\frac{1}{2}}} r_{I,J-\frac{1}{2}} \cos\phi_{I,J-1} - N_{\phi_{I,J+\frac{1}{2}}} r_{I,J+\frac{1}{2}} \cos\phi_{I,J} \right.$$

$$\left. + Q_{\phi_{I,J+\frac{1}{2}}} r_{I,J+\frac{1}{2}} \sin\phi_{I,J} - Q_{\phi_{I,J-\frac{1}{2}}} r_{I,J-\frac{1}{2}} \sin\phi_{I,J-1} \right]$$

where ℓ_{57} is the length of the shell segment 57. The zone pressures ($P_{I,J}$, $P_{I-1,J}$, $P_{I,J-1}$, and $P_{I-1,J-1}$) are obtained from the hydrodynamic calculation.

The transverse shear force $Q_{\phi_{I,J-\frac{1}{2}}}$ is calculated from eq. (17), in finite-difference form,

$$Q_{\phi_{I,J-\frac{1}{2}}} = \frac{1}{r_{I,J-\frac{1}{2}}} \left[\frac{M_{\phi_{I,J}} r_{I,J} - M_{\phi_{I,J-1}} r_{I,J-1}}{\ell_{oc}} \right.$$

$$\left. - M_{\phi_{I,J-\frac{1}{2}}} \cos\phi_{I,J-1} \right] \tag{35}$$

where ℓ_{oc} is the length of the shell segment OC.

(b) Circular Plate

Let the J line in fig. 2. be the middle plane of the bottom plate. The acceleration in the r direction is given by eq. (15), in finite-difference form,

$$\ddot{r}_{I,J} = \frac{1}{m_{68}}\left[N_{\phi_{I+\frac{1}{2},J}} r_{I+\frac{1}{2},J} \cos\psi_{I,J} - N_{\phi_{I-\frac{1}{2},J}} r_{I-\frac{1}{2},J} \cos\psi_{I-1,J} - Q_{\phi_{I+\frac{1}{2},J}} r_{I+\frac{1}{2},J} \sin\psi_{I,J}\right.$$

$$\left. + Q_{\phi_{I-\frac{1}{2},J}} r_{I-\frac{1}{2},J} \sin\psi_{I-1,J} - \frac{\ell_{68}}{2}\left(N_{\theta_{I+\frac{1}{2},J}} + N_{\theta_{I-\frac{1}{2},J}}\right)\right] \qquad (36)$$

where m_{68} and ℓ_{68} are the mass and length of the plate segment 68, and $\psi_{I,J}$, $\psi_{I-1,J}$ are, respectively, the angle of inclination of the elements OD and BO with respect to the r direction. The acceleration in the z direction is given by

$$\ddot{z}_{I,J} = \frac{1}{(A\rho)_{I,J}}\left[(P_{I,J} - P_1 - P_{I-1,J-1})(r_{I,J+1} - r_{I,J-1} + r_{I-1,J} - r_{I+1,J})\right.$$

$$\left. - (P_{I-1,J} - P_2 - P_{I,J-1})(r_{I,J+1} - r_{I,J-1} + r_{I+1,J} - r_{I-1,J})\right] \qquad (37)$$

where the strength of the plate is represented by two equivalent pressures P_1 and P_2. If the strength of the plate is ignored, i.e., $P_1=P_2=0$, eq. (37) reduces to eq. (30). The pressures P_1 and P_2 are calculated from

$$P_1 = \frac{N_{\theta_{I+\frac{1}{2},J}} \sin\psi_{I,J}}{r_{I+\frac{1}{2},J}} + P_{12}$$

$$P_2 = \frac{N_{\theta_{I-\frac{1}{2},J}} \sin\psi_{I-1,J}}{r_{I-\frac{1}{2},J}} + P_{12}$$

$$P_{12} = \frac{1}{\ell_{68} r_{I,J}}\left[N_{\phi_{I+\frac{1}{2},J}} r_{I+\frac{1}{2},J} \sin\psi_{I,J} - N_{\phi_{I-\frac{1}{2},J}} r_{I-\frac{1}{2},J} \sin\psi_{I-1,J}\right.$$

$$\left. + Q_{\phi_{I+\frac{1}{2},J}} r_{I+\frac{1}{2},J} \cos\psi_{I,J} - Q_{\phi_{I-\frac{1}{2},J}} r_{I-\frac{1}{2},J} \cos\psi_{I-1,J}\right]$$

where ℓ_{68} is the length of the plate segment 68. The zone pressures ($P_{I,J}$, $P_{I-1,J}$, $P_{I,J-1}$, and $P_{I-1,J-1}$) are obtained from the hydrodynamic calculation. The transverse shear force Q_ϕ is calculated from eq. (17).

3. SAMPLE PROBLEM

The problem chosen for REXCO-H analysis was a liquid sodium cooled fast reactor shown in fig. 3. The core oxide fuel was contained in stainless steel pins supported in a steel grid. The core was surrounded by a radial reflector, radial shield, an upper axial reflector and plenum, and a lower axial reflector and shield. The sodium was blanketed with

inert gas and was contained in a steel vessel. The vessel was installed within a concrete cavity that had a rotating shield plug at the top. The plug was fastened to the ground by holddown bolts. Because of the axisymmetry only half the cross section is shown in fig. 3.

It was assumed that after core disassembly excursion, the fuel was fragmented and dispersed into the core sodium causing a rapid transfer of heat to the sodium followed by an energetic expansion of sodium vapor. The sodium had a peak pressure of 2.03 kbar, and a work energy of 350 Mw-sec when it was expanded to 1 atm pressure.

Fig. 4. shows that the magnitude of the pressure decreases as the shock wave propagates through the core into the surrounding media. The grid deformations at various times are shown in fig. 5. At time t = 22.102 msec, the sodium slug has been pushed upward, contacting the top shield plug, by the core sodium vapor. The deformations of the vessel occur mostly around the reactor core region with a maximum strain of 5.2%.

Next, the REXCO-H code was used to examine the slug impact force and the deformations of the upper vessel wall. When the sodium slug contacted the rotating shield plug, the sodium slug was assumed moving with a velocity of 89 ft/sec and having a total kinetic energy of 43.6 Mw-sec. Detail velocity distribution is available from the computer outputs. However, for the sake of illustration, a uniform velocity field was used in the analysis. The pressure in the core vapor was only 200 psig at the time of impact. Fig. 6. shows the slug force acting on the rotating plug and the partitioning of various energies, both as a function of time. The slug force consists of a large triangular shape impulse, which lasts for about 2 msec, and a long-duration oscillating residual pressure force, which lasts for about 30 msec. The energy curves show how energy is converted from axial kinetic energy into internal energy of coolant, radial kinetic energy of coolant, vessel strain energy, and energy of head and bolts. Fig. 7. shows the typical velocity and displacement curves of the upper vessel wall in a slug impact accident.

4. SUMMARY COMMENTS

The accuracy of the present numerical method has been evaluated by comparison with experimental results by Ash and Julke [6]. Four sets of experiments were analyzed. Each test case consisted of a model experiment in which the excursion energy release was simulated by the detonation of a chemical high-explosive charge. The results of the comparisons indicate that the REXCO-H code can be applied directly to certain containment problems involved in reactor safety. Not only can experimental data be reproduced with such a computer code, but also detailed insights can be gained into the relative effects of parameter variations through the use of the code. Optimal containment design for safety requires a wide range of quantitative measures of the relative performance of materials and structural configurations. Through the use of computer code initial conditions can be varied easily to simulate possible accident situations, and the effects of design modifications can be assessed far more quickly and economically than by means of building and testing scale models.

REFERENCES

[1] Von Neumann, J., Richtmyer, R. D., "A Method for the Numerical Calculation of Hydrodynamic Shocks", J. Appl. Physics 21, No. 3, 232-237 (1950).

[2] Murnaghan, F. D., "The Compressibility of Media Under Extreme Pressures", Proc. Nat. Acad. Sci. 30, 244-247 (1944).

[3] Richtmyer, R. D., Morton, K. W., Difference Methods for Initial Value Problems, p. 350, 2nd Edition, Interscience Publishers, Inc., New York (1967).

[4] Chang, Y. W., Gvildys, J., Fistedis, S. H., "Hydrodynamic Response of Primary Reactor Containment to High-energy Excursions", Nucl. Eng. Design 12, 344-360 (1970).

[5] Chang, Y. W., Gvildys, J., Fistedis, S. H., Two-dimensional Hydrodynamics Analysis for Primary Containment, ANL-7498 (November 1969).

[6] Ash, J. E., Julke, R. T., Comparison of a Two-dimensional Hydrodynamics Code (REXCO) to Excursion Experiments for Fast Reactor Containment, ANL report (to be published).

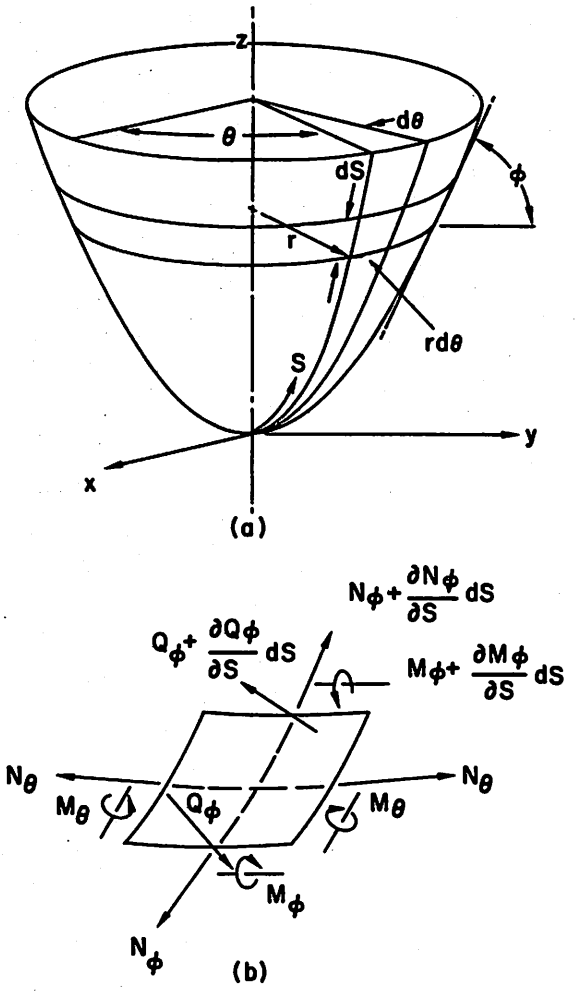

1. Nomenclature for a Shell of Revolution

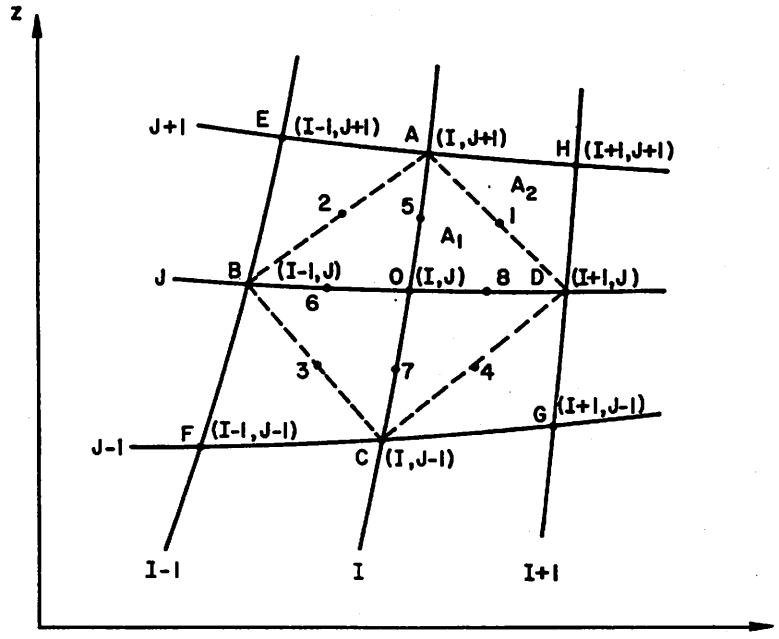

2. A Typical Mesh Point, (I,J), with Adjacent Zones and Points, Illustrating the Notation used in Finite-difference Equations

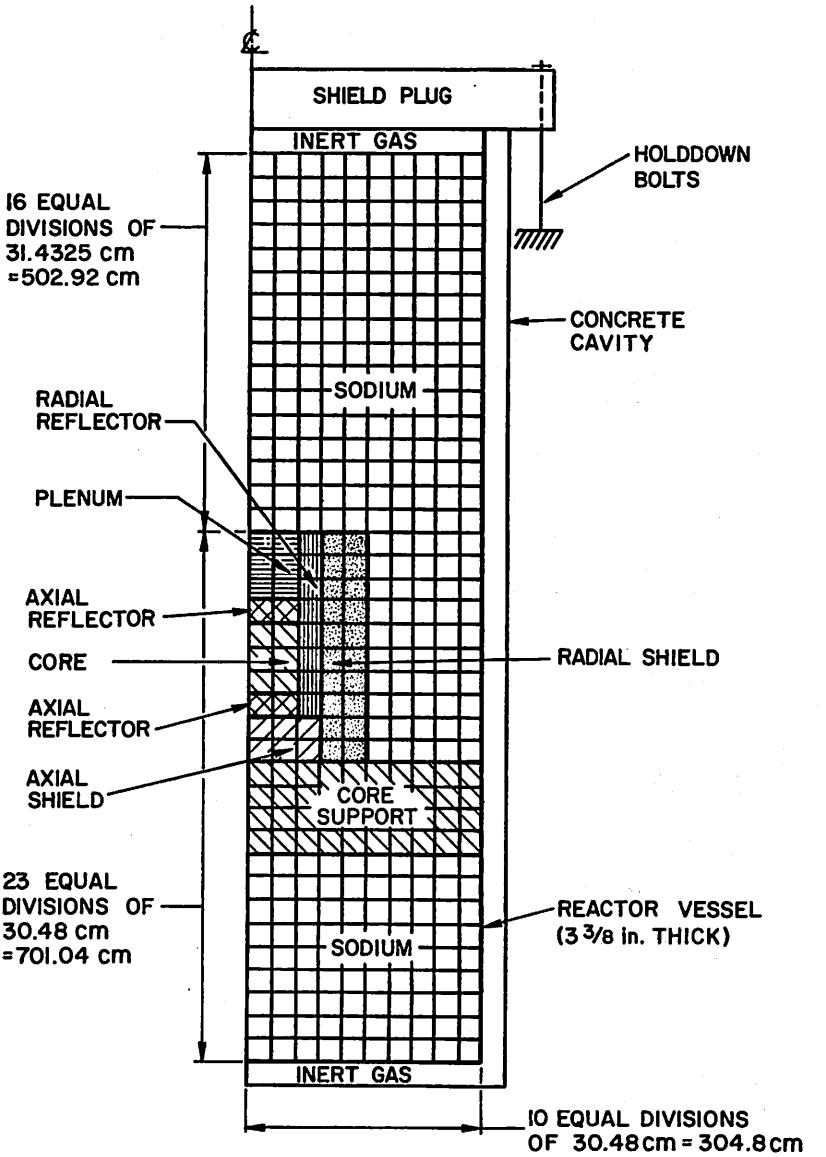

3. The Reactor Model as used in the REXCO-H Analysis

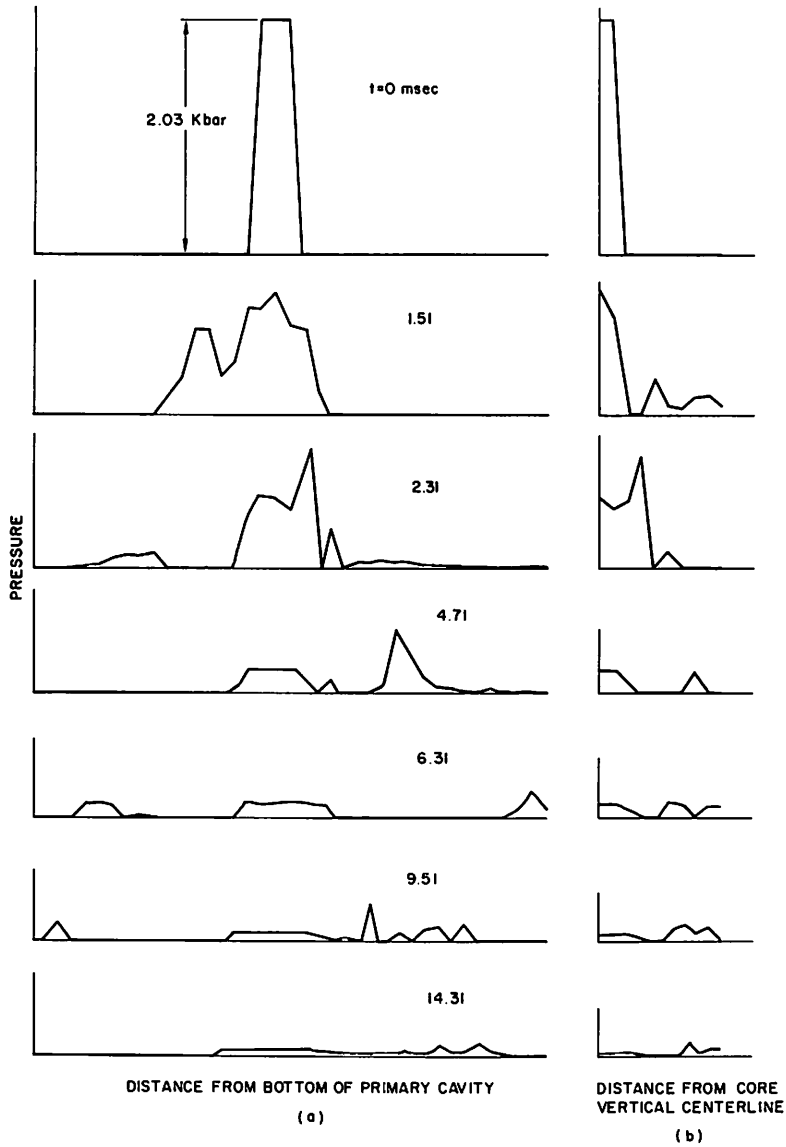

4. Pressure Profiles at Various Times: (a) along Core Vertical Centerline; (b) along Core Horizontal Axis

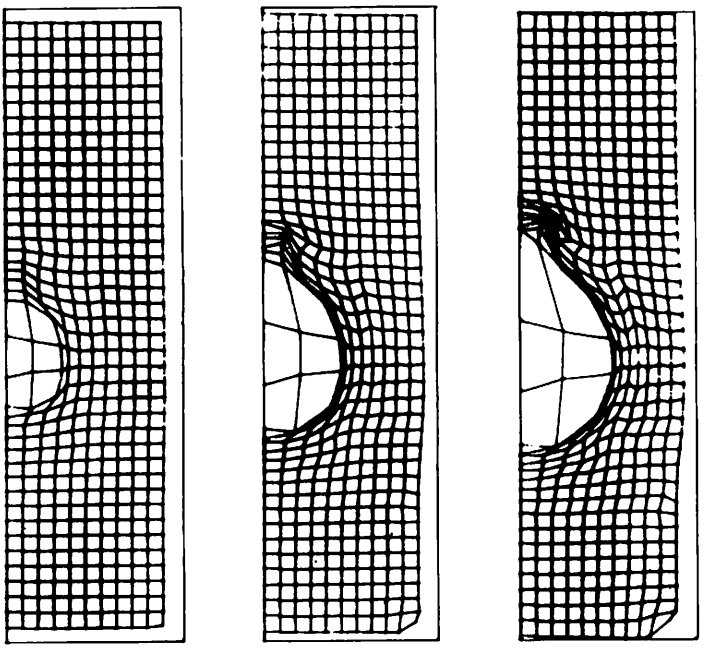

5. Deformation of Lagrangian Grids at Various Times

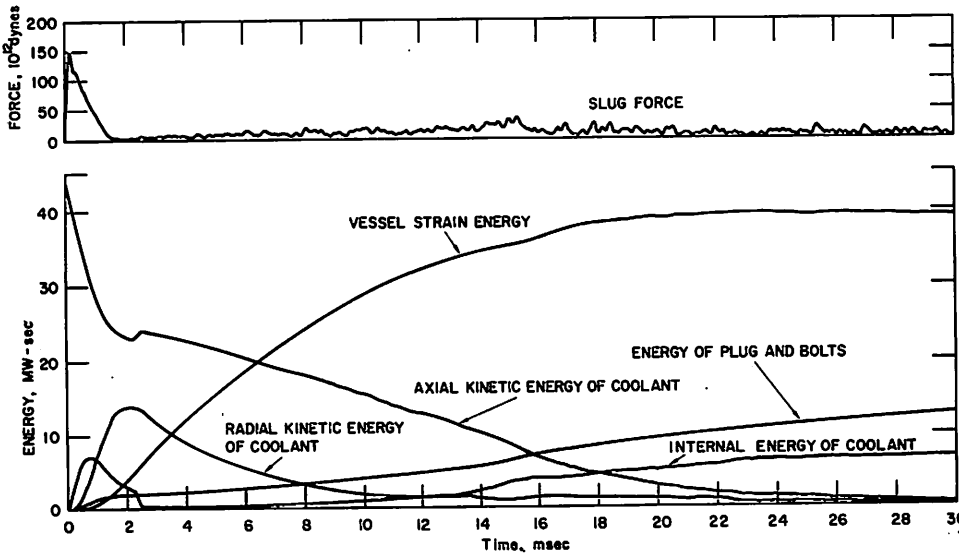

6. Impact Force Acting on the Rotating Plug and Partitioning of Various Energies

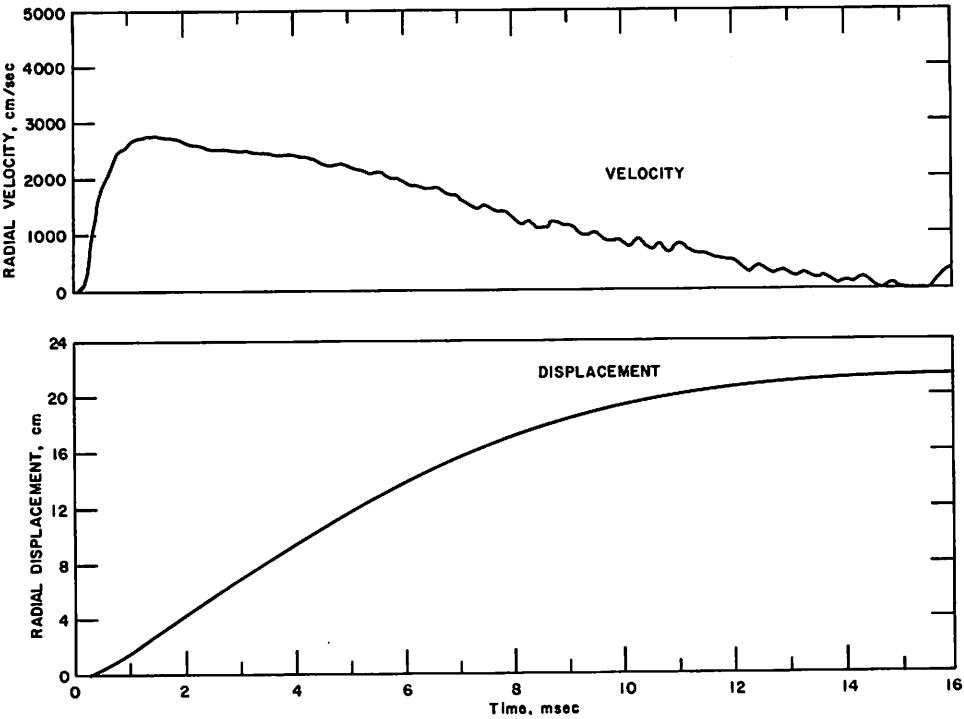

7. Typical Velocity and Displacement Curves of the Upper Vessel Wall in a Slug Impact Accident